Research article

Conditional reprogrammed human limbal epithelial cell model for anti-SARS-CoV-2 drug screening

Yu Xiao [a,d], Ling Wang [c], Shi-xu Li [c], Shi-song Fang [e], Fan Luo [b], Shu-liang Chen [b], Xuan Zou [e,**], Lin Ye [c,***], Wei Hou [a,b,*]

[a] Shenzhen Research Institute, Wuhan University, Shenzhen 518057, Guangdong Province, China
[b] State Key Laboratory of Virology/Institute of Medical Virology, School of Basic Medical Sciences, Wuhan University, Wuhan 430071, Hubei Province, China
[c] Shenzhen Eye Hospital, Shenzhen 518040, Guangdong Province, China
[d] Department of Clinical Laboratory, The Seventh Affiliated Hospital of Sun Yat-Sen University, Shenzhen, 518107, China
[e] Shenzhen Center for Disease Control and Prevention, Shenzhen 518055, Guangdong Province, China

A B S T R A C T

To minimize the global pandemic COVID-19 spread, understanding the possible transmission routes of SARS-CoV-2 and discovery of novel antiviral drugs are necessary. We describe here that the virus can infect ocular surface limbal epithelial, but not other regions. Limbal supports wild type and mutant SARS-CoV-2 entry and replication depending on ACE2, TMPRSS2 and possibly other receptors, resulting in slight CPE and arising IL-6 secretion, which symbolizes conjunctivitis in clinical symptoms. With this limbal model, we have screened two natural product libraries and discovered several unreported drugs. Our data reveal important commonalities between COVID-19 and ocular infection with SARS-CoV-2, and establish an ideal cell model for drug screening and mechanism research.

1. Introduction

COVID-19 caused by SARS-CoV-2 infection promotes multiple symptoms in several systems, including the respiratory, gastrointestinal, hepatic, ocular, and cardiovascular. Anosmia, the loss of smell, is a common and often the sole symptom of COVID-19 [1]. During the 2020–2021 COVID-19 pandemic period, the mortality and life expectancy in 204 countries and territories and 811 additional subnational locations displayed terrible changes [2]. And in previously well individuals with mild initial COVID-19 illness, 73 % of participants reported cardiac symptoms, such as exertional dyspnea (62 %), palpitations (28 %), atypical chest pain (27 %) and syncope (3 %) [3]. Investigators have isolated viable virions from contaminated surfaces, including dry surfaces and frozen fish, and have proved that virus infection can occur via the fomite transmission route [4]. The long-term viability of SARS-CoV-2 makes it possible to transmit via aerosol and fomite, and this transmission commonly occurs in health-care workers or hospital areas [5].

Mechanistically, face coverings can act as a protection against respiratory infection by reducing upper respiratory tract exposure to a virus. However, a study based on 10 cases about COVID-19 post-mortem human ocular tissues discovered viral NP existed in conjunctiva, anterior cornea, posterior cornea and vitreous [6–8]. In addition, conjunctivitis has been reported as a typical symptom of COVID-19, and SARS-CoV-2 RNA has been detected in quite a lot of positive patients' conjunctival tear film (0–10 %) [9–11]. A recent case report found a female patient suffered Bilateral Acute Depigmentation a month after being diagnosed with COVID-19 [12]. In addition, a Meta-Analysis confirmed that COVID-19 pandemic brought a significantly higher prevalence of dry eye than before [13]. Eye, especially in the ocular surface, can be infected by SARS-CoV-2 and display multiple ophthalmic manifestations caused by COVID-19 [14–16].

Normal ocular tissues, particularly ocular surface limbal, cornea and conjunctiva regions can express both ACE2 and TMPRSS2, which enables SARS-CoV-2 entry [17]. To determine the most susceptible area and potential infection route in ocular, we used human primary ocular epithelial cells isolated from healthy donors for SARS-CoV-2 study. The cells were cultured by Conditional Reprogramming (CR) technology to ensure they were highly proliferative and maintain their original karyotypes without transfect other proteins [18]. We also evaluated the infectivity of ocular cells, bronchial epithelial cells and Vero cells. Of all ocular cells only three limbal epithelial cells support SARS-CoV-2 entry and replication, although others also express ACE2 and TMPRSS2. Moreover, TMPRSS2 inhibitor did not show the due anti-viral effect in limbal, which illustrated there may be other receptors participating in ocular infection. We thereby established a SARS-CoV-2 infection cell model and discovered various compounds as effective antiviral drugs against COVID-19.

2. Materials and methods

2.1. Cell lines and conditional reprogramming human primary cell culture

Vero cells (kidney epithelial cells from female African green monkey, CSTR:19375.09.3101MONGNO10) were maintained in Dulbecco's Modified Eagle Medium (DMEM, GIBCO) supplemented with 10 % FBS (Biological Industries) and 1 % penicillin/streptomycin (GIBCO) at 37 °C in a humidified atmosphere with 5 % CO_2. HNRPE2 was maintained in DMEM/F12 -Dulbecco's Modified Eagle Medium (GIBCO) supplemented with 10 % FBS (Biological Industries) and 1 % penicillin/streptomycin (GIBCO) at 37 °C in a humidified atmosphere with 5 % CO_2.

Globes from human donors aged between 36 and 90 years were obtained from the Eye-Bank for Shenzhen Eye Hospital. For conditional reprogramming human primary cell culture, eye tissues were isolated from globes and established several human normal epithelial cells with long lifespan and physiological function for toxicity and virology research. Cell isolation and conditional reprogramming (CR) culture were conducted according to previous report [19]. The genome DNA of human limbal epithelial cells was isolated with the kit (Cat:DP304, Tiangen, Beijing, China). Short tandem repeat (STR) analysis (DNA fingerprinting) was performed by commercial kit (Powerplex 21 system; Promega Corporation, Madison, WI) [20]. This research had been approved by the ethics committee of Shenzhen Eye Hospital (2023KYPJ010).

2.2. Virus isolation

SARS-CoV-2 was isolated from throat swabs of COVID-19 patients and propagated in Vero cells cultured in Dulbecco's Modified Eagle Medium (DMEM, GIBCO) supplemented with 2 % FBS (Biological Industries) and 1 % penicillin/streptomycin (GIBCO) at 37 °C in a humidified atmosphere with 5 % CO_2. Cell flasks were frost thawing twice in −80 °C before harvested virus, and virus stock was stored in −80 °C after filtration through a Millipore Express PES Membrane filter unit (0.22 μm). Virus isolation and propagation were operated in Shenzhen Center for Disease Control and Prevention.

2.3. Viral infection

Plates containing different cells were transferred into BSL-3 Lab before SARS-CoV-2 infection, and then the diluted viruses were added and incubated with cells at 37 °C for 1 h. After that, the virus were wash off three times with Phosphate Buffered Saline (PBS) at room temperature, and then cultured with fresh 2 % FBS DMEM for Vero cells, or primary epithelial culture basic medium (PECBM) for CR-human primary cells.

2.4. Immunofluorescence staining

Cells were fixed with 4 % paraformaldehyde (PFA) at 4 °C for 48 h, rinsed three times with PBS, then incubated with TritonX-100 (Solarbio, P1080) at room temperature for 20 min to permeabilize cells. Block non-specific reaction with 10 % FBS PBS at room temperature for 1 h, and resuspend primary antibody in 5 % BSA PBS overnight at 4 °C. Cells were rinsed three times and incubated with the appropriate fluorochrome-conjugated secondary antibodies and DAPI (ab285390) at room temperature for 1 h, then washed out antibodies and DAPI with PBS for three times before taking images using an Axio Observer 3 (Zeiss)microscopy [21]. Goat Anti-Rabbit IgG H&L (Alexa Fluor® 488, ab150077), Goat Anti-Mouse IgG H&L (Alexa Fluor® 488, ab150113), Goat Anti-Mouse IgG H&L (Alexa Fluor® 647, ab150115) and Goat Anti-Rabbit IgG H&L (Alexa Fluor® 647, ab150079) were purchased from the Abcam.

2.5. SARS-CoV-2 spike mediated cell-cell fusion

HEK293 cells plated in 60-mm culture dish were transfected with 10 μg pcDNA3.1-GFP or pcDNA3.1-Spike-GFP (Miaolingbio) at 30 % confluence. After two days' transfection, resuspended the HEK293 cells and co-cultured with HNCEC/HL-008 or Vero cells at a
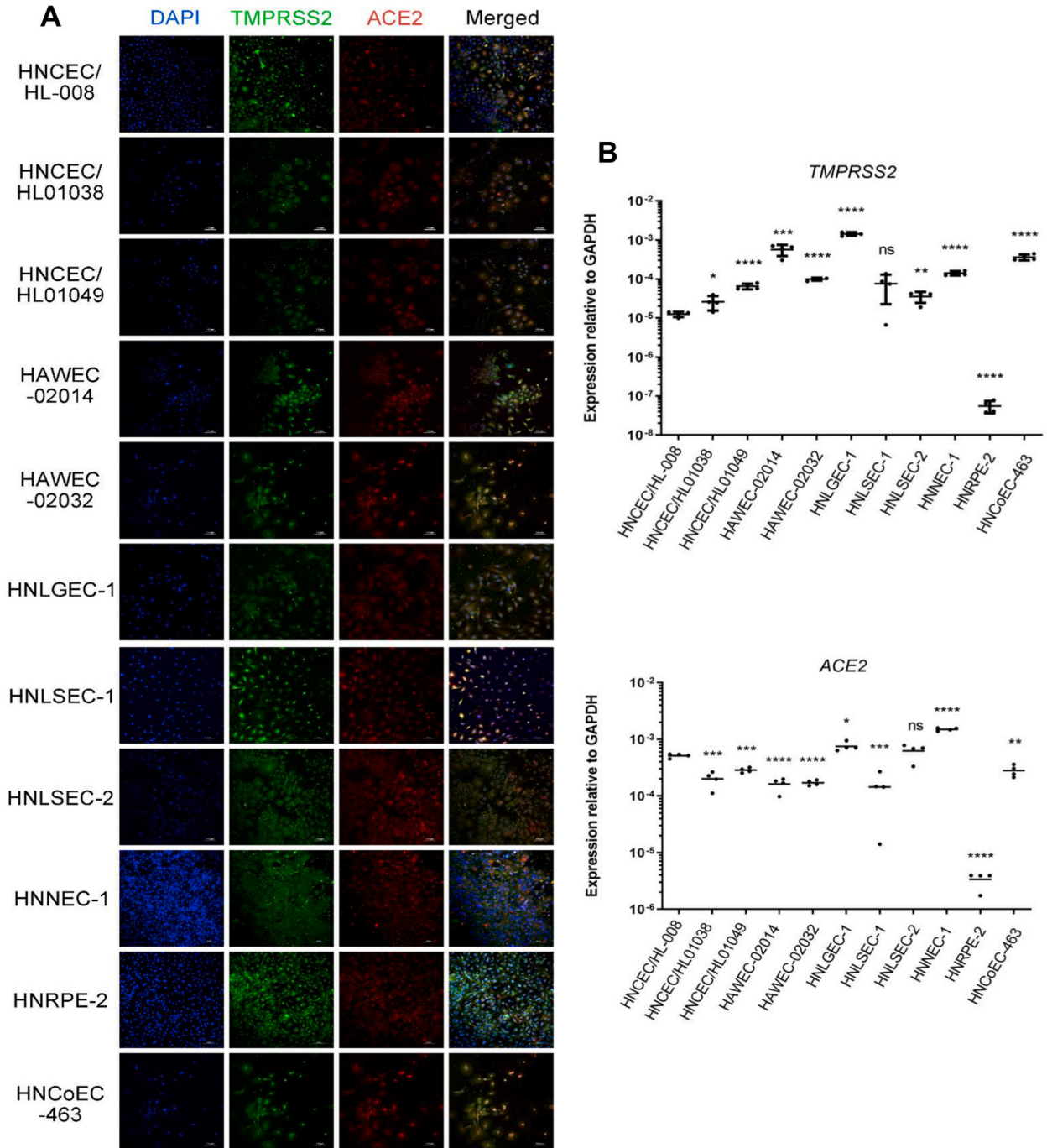

Fig. 1. Expression of ACE2 and TMPRSS2 in primary human epithelial cells isolated from human eyes. A. Three limbal epithelial cells (HNCEC/HL-008, HNCEC/HL01038 and HNCEC/HL01049), two human normal bronchial epithelial cells (HAWEC-02014 and 02032), two lacrimal sac epithelial cells (HNLSEC-1 and 2), one lacrimal gland epithelial cell (HNLGEC-1), one nasolacrimal duct epithelial cell (HNNEC-1), one conjunctiva epithelial cell (HNCoEC-463) and one retina (HNRPE-2) were fixed with 4 % PFA and then strained with antibodies against human ACE2 and TMPRSS2. Scale bar: 100 μm. B. qRT-PCR for ACE2, TMPRSS2 and GAPDH with total RNA extracted from epithelial cells. Significance analysis data was showed in Supplementary Materials. *adjusted p < 0.05, **adjusted p < 0.01, ***adjusted p < 0.001, ****adjusted p < 0.0001 (Student *t*-test).
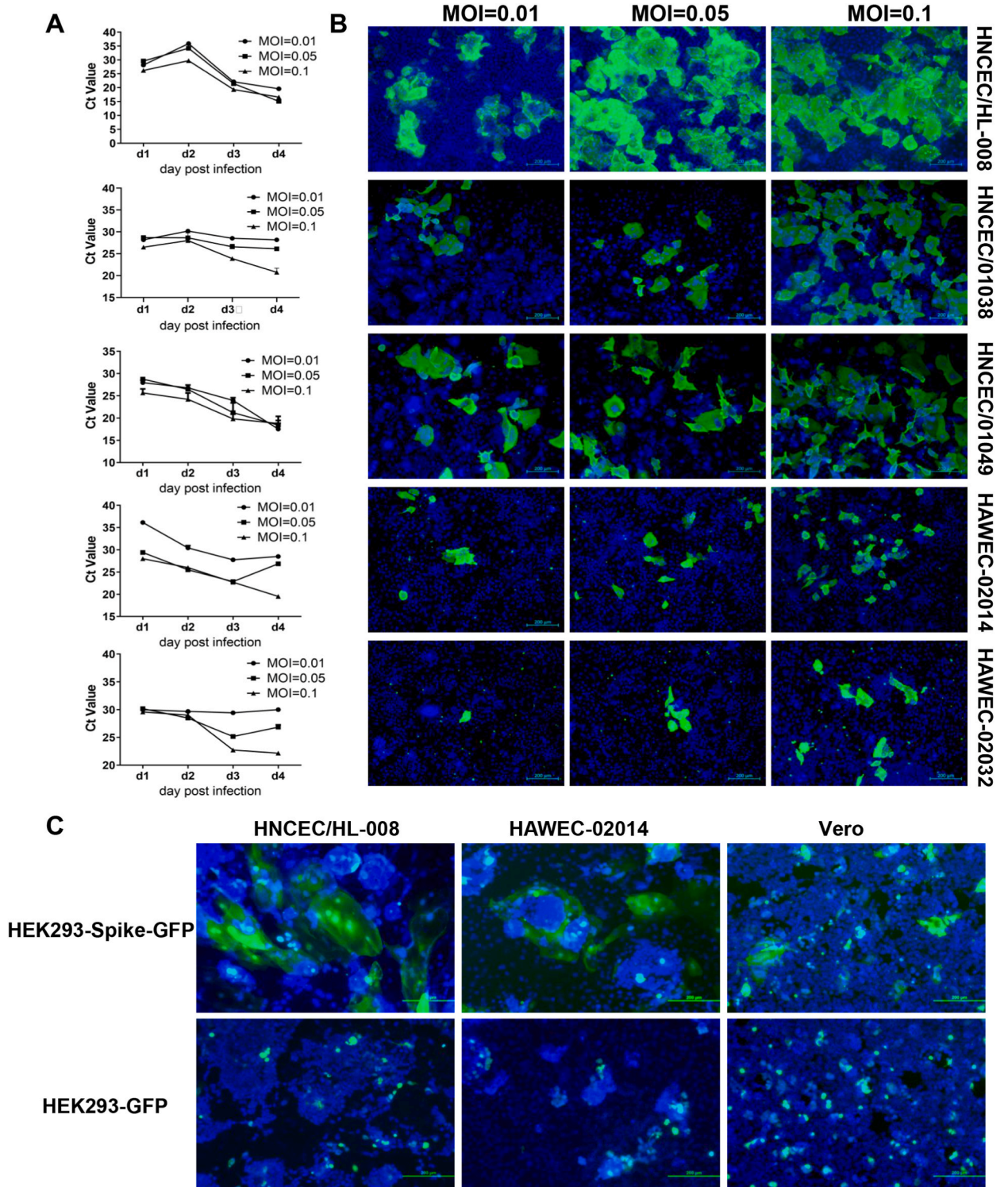
3

Fig. 2. Sensitivity of conditional reprogrammed human limbal epithelial cells and human airway epithelial cells to SARS-CoV-2 infection. A and B. Conditional reprogrammed human limbal epithelial cells and human airway epithelial cells were infected with WIV-04 strain of SARS-CoV-2 for 4 days. The transcript of SARS-CoV-2 spike gene in supernatant and the expression of SARS-CoV-2 nucleocapsid (NP) in cells were measured by RT-qPCR (A) and Immunofluorescence assay (B) respectively. Scale bar: 200 μm. C. Syncytia formation by fusion of SARS-CoV-2 spike expressing HEK293 cells and ACE2-expressing cells. HNCEC/HL-008, HAWEC-02014 and Vero cells were co-cultured with SARS-CoV-2 Spike-GFP expressing HEK293 or GFP expressing HEK293 cells at rate 2:1 for 96 h, and then fixed with 4 % PFA and strained with DAPI for microscope observation Scale bar: 200 μm.

rate of 1:2, and analyzed the fluorescence signal after four days' co-culture.

2.6. Western blot

Cells in 24- well plates were lysed with 200 μL lysate buffer [10 mM Tris-HCl (pH 7.6), 0.1 % NP-40, 100 mM NaCl, and 1 mM EDTA] (contained 1 mM PMSF) at 4 °C for 30 min and added with 50 μL 5x SDS loading buffer (Beyotime, P0015) before boiling at 100 °C in a Dry Bath Incubator. Protein samples were resolved by SDS-polyacrylamide gel electrophoresis and transferred onto a polyvinylidene difluoride (PVDF) membrane using Trans-Blot Turbo Transfer System (Bio-Rad, Hercules, CA), followed by blocking for 1 h and probing with an indicated primary antibody and an anti-Rabbit/Mouse IgG-HRP antibody (Beyotime, A0208 and A0216) [21]. The proteins were visualized using SuperSignal West Pico Plus Stable Peroxide Solution (Lot:TK275825) and Luminol/Enhancer Solution (Lot:UA276944). Anti-SARS-CoV-2 spike glycoprotein was purchased from abcam (ab272854). SARS-CoV/SARS-CoV-2 Nucleocapsid Antibody was purchased from SinoBiological (40143-R001). Human ACE2 antibody (ab272500), TMPRSS2 antibody (ab280567), Cytokeratin 19 antibody (ab76539), RPE65 antibody (ab238712), p63 antibody (ab124762), Aquaporin 5 antibody (ab92320) and GAPDH antibody (ab8245) were purchased from abcam.

2.7. Quantitative real-time PCR (qRT-PCR) analysis

RNA in the cell culture supernatant was extracted with Libex 96 (qEx-DNA/RNA, T183X) and used for reverse transcription by PrimerScript RT Master Mix (Takara, Lot:AN82328A). qRT-PCR was performed on a CFX Connect (Bio-rad) using iTaq Univer SYBR qPCR Mix Kit (Bio-rad, Lot: 172512) and primers specific for SARS-CoV-2 Spike subgenomic RNA, ACE2, TMPRSS2, IL-6, IL-8 and GAPDH were listed in the supplementary materials [22].

2.8. Inflammatory factors detection by enzyme linked immunosorbent assay (ELISA)

Cell supernatant containing viruses was heated at 60 °C for 45 min in a Dry Bath Incubator before taking away from BSL-3 lab. The ELISA kit of Human IL-6 was purchased from BD biosciences (Cat:550799), ELISA kits for IL-8 (Cat:KE00006), IL-18 (Cat:KE00025), IL-21 (Cat:00022), IL-27 (Cat:00182) were purchased from Proteintech. The ELISA kit of human IL-33 (Cat:SEB980Hu) was purchased from Cloud-Clone Corp. Detection of inflammatory factors was conducted according to the Description of products.

2.9. Cytotoxicity assay and drug screening

Cells were seeded in 96-well plates at a density of 1.0×10^4 cells per well. After 24 h, cells with 80 % confluence were added with a series of concentration gradient of compound and cultured for an additional 48 h or 96 h. The supernatants were removed and the cells were washed three times with PBS. Finally, the cells in each well were incubated with 100 μL of diluted Cell Counting Kit-8 reagent at 37 °C for 1 h. The fluorescence was measured using a PerkinElmer Envision Multi label Plate Read. For drug screening, Drug Library HY-L021 and HY-L021L were purchased from MedChemExpress, containing over 3000 natural products structurally like compounds for high througout screening (HTS) and high content screening (HCS). Vero and HNCEC/HL-008 were infected with Delta at MOI = 0.05 and were incubated with diluted compounds. Cells were strained by antibody to NP at 48.hpi (48.hpi for Vero and 96.hpi for HNCEC/HL-008) and photographed using Axio Observer 3 (Zeiss)microscopy. The two libraries were screened for 3 rounds at concentration gradient to avoid False-Positives caused by cytotoxicity or operating error.

3. Results

3.1. Assessment of human normal primary ocular epithelial cells isolated from clinical surgery

We obtained normal human limbal, conjunctival, lacrimal gland, lacrimal sac, nasolacrimal duct and bronchial epithelial cells separated from the eye globe or clinical surgery, and then isolated primary epithelial cells by a Conditional reprogramming (CR) technique [19]. CR-limbal epithelial cells and CR-bronchial epithelial cells had been identified in our previous research [20,23]. The expression of tissue specific marker and p63 in lacrimal gland, lacrimal sac, nasolacrimal duct epithelial and retina cells was displayed in Supplementary fig. 1 and Figure.2 [24]. Immunofluorescence results showed all primary epithelial cells displayed both ACE2 and TMPRSS2 expression, including three limbal epithelial cells (HNCEC/HL-008, HNCEC/HL01038 and HNCEC/HL01049), two bronchial epithelial cells (HAWEC-02014 and 02032), one lacrimal gland epithelial cell (HNLGEC-1), two lacrimal sac epithelial cells (HNLSEC-1 and 2), one nasolacrimal duct epithelial cell (HNNEC-1), one conjunctiva epithelial cell (HNCoEC-463) and one retina (HNRPE-2) (Fig. 1A). Contrast to other ocular cells, limbal epithelial cells showed comparatively low TMPRSS2, and bronchial epithelial cells seemed to exhibit superior TMPRSS2 (Fig. 1B). Data from these experiments suggest that the human ocular surface may act as a potential route of SARS-CoV-2 transmissions for both ACE2 and TMPRSS2 adequately [25,26].
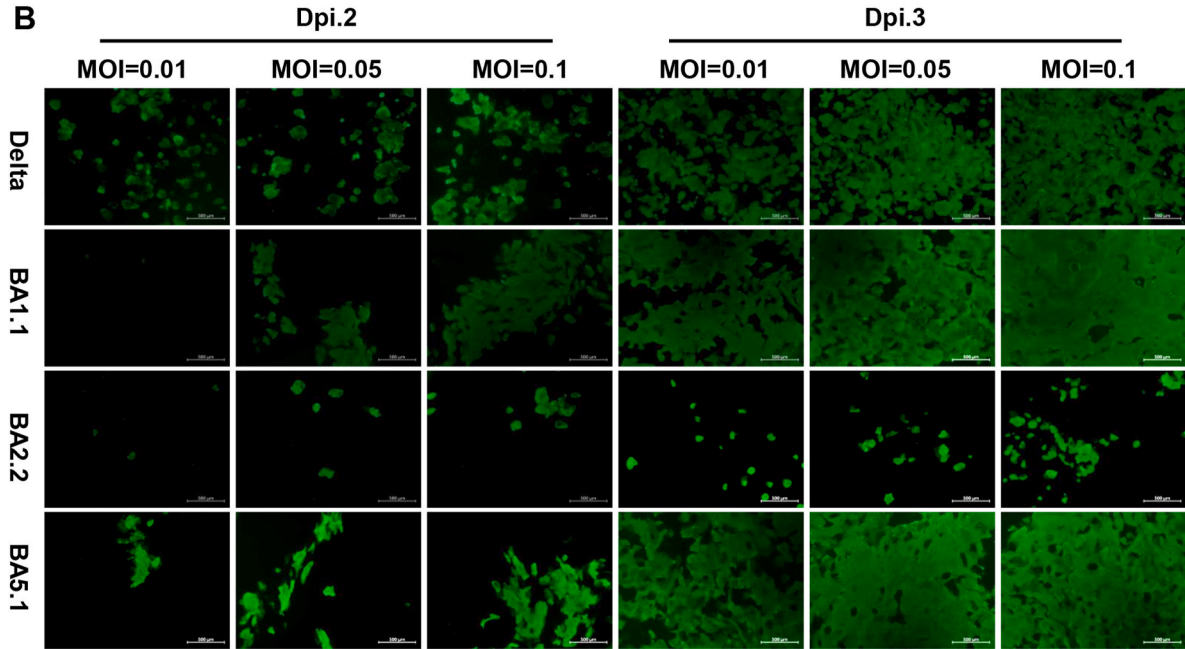
3.2. Comparison of different types of ocular cells to SARS-CoV-2 infection

In order to evaluate whether the expression of ACE2 and TMPRSS2 was consistent with the susceptibility to SARS-CoV-2 infection in these primary ocular epithelial cells, all of these cells were infected with SARS-CoV-2 WIV-04 strain at a multiplicity of infection
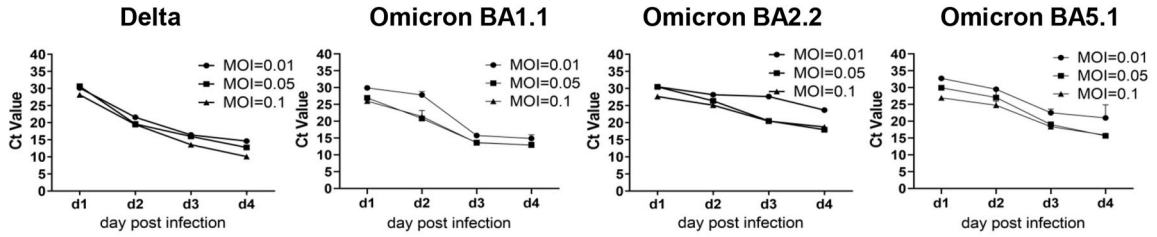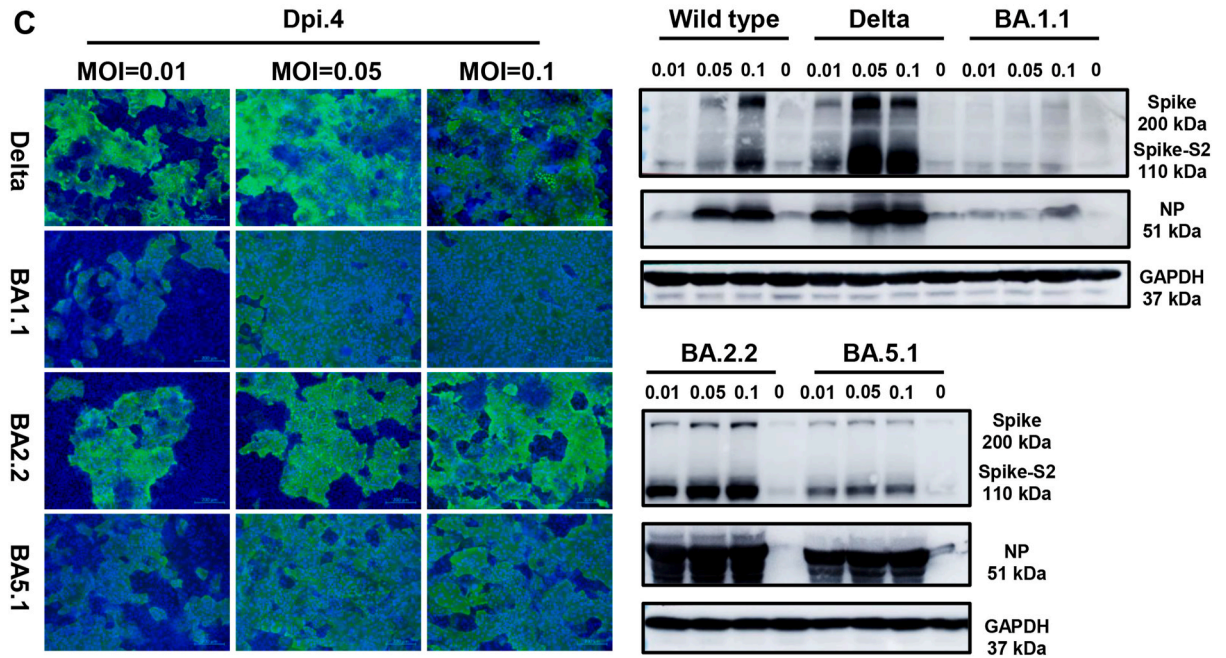
(caption on next page)

Fig. 3. Susceptibility of SARS-CoV-2 variants infection of HNCEC/HL-008. A. HNCEC/HL-008 infected with mutant strains for 4 days, detected SARS-CoV-2 subgenomic spike transcript in supernatant by RT-qPCR and plotted replication curves. B. Cells in A were immunoblotted with antibody against nucleocapsid of SARS-CoV-2at dpi. 2 and dpi. 3, and photographed by fluorescence microscope at Objective 4x. Scale bar:500 μm. C. Cells in A were immunoblotted with antibody against nucleocapsid of SARS-CoV-2 and strained with DAPI for fluorescence microscope observation at dpi.4 (Objective 10x). The expression of nucleocapsid (SARS-CoV-2) and spike (SARS-CoV-2) were analyzed with Western Blot. The full, non-adjusted images were displayed in the supplementary material 2 (Figure.1). Scale bar: 200 μm.
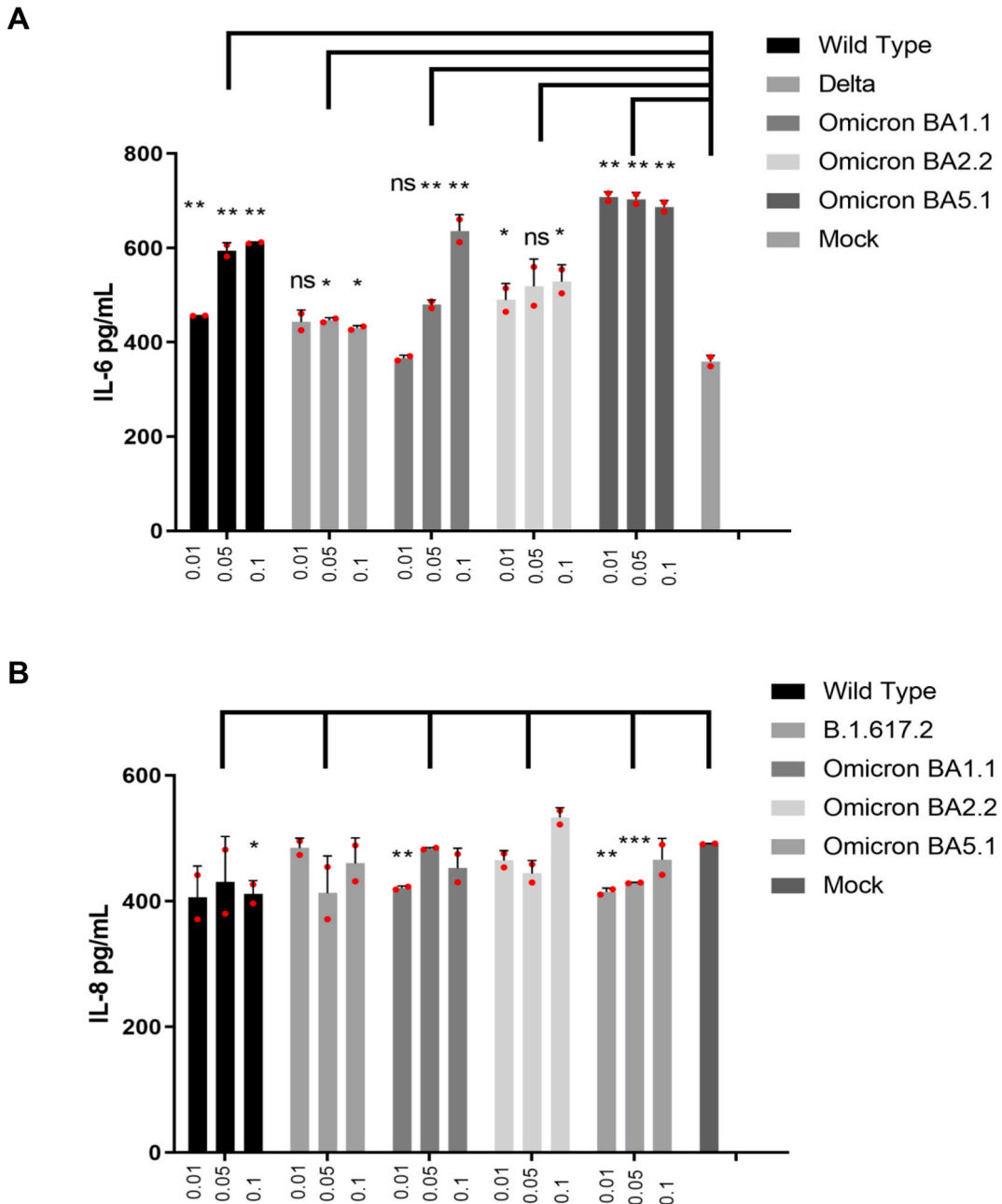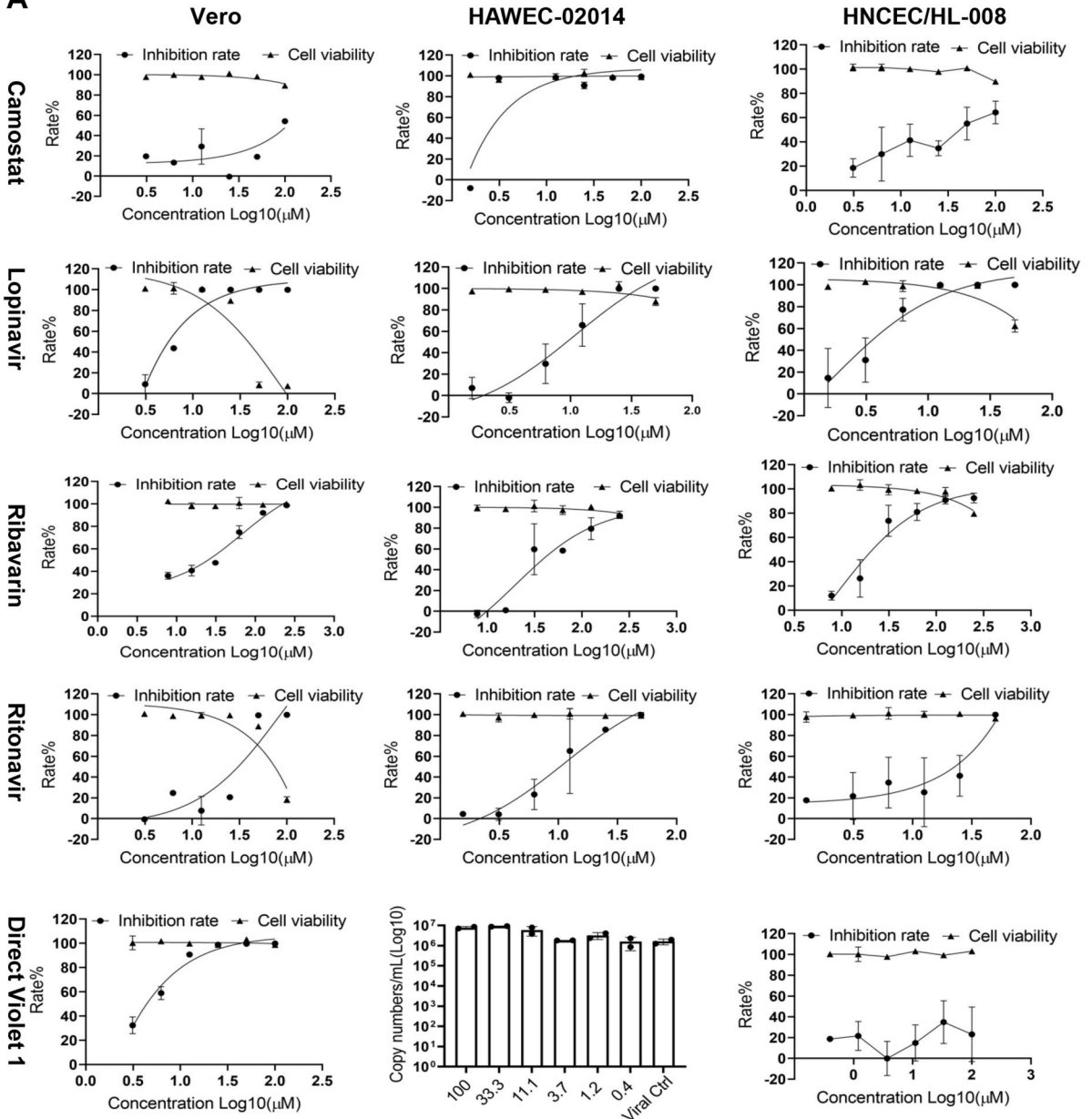

Fig. 4. SARS-CoV-2 infection of HNCEC/HL-008 induces IL-6 secretion. A and B HNCEC/HL-008 cells were infected with WIV-04 strain or mutant strains of SARS-CoV-2 at different MOI, then detected supernatant IL-6 (A) and IL-8 (B) by ELISA.
Significance analysis data was showed in Supplementary Materials. *adjusted $p < 0.05$, **adjusted $p < 0.01$(Student *t*-test).

A

B

	Vero	HAWEC-02014	HNCEC/HL-008
Camostat	NS	7.56	>50
Lopinavir	12.15	11.03	5.667
Ribavarin	66.55	11.82	9.07
Ritonavir	12.35	11.26	25.83
Direct Violet 1	3.166	NS	NS

IC50 of drugs in different cell lines
Concentration unit: μM

(caption on next page)

Fig. 5. Antiviral effect of five reported positive drugs in different cell models. A. Vero (right), HAWEC-02014 (middle) and HNCEC/HL-008 (left) cells were pretreated with diluted drugs for 2 h before viral infection, then incubated with Delta virus for 48 h (Vero) or 96 h (HAWEC-02014 and HNCEC/HL-008). The inhibition rate was analyzed by qRT-PCR of spike transcript in supernatant and graphed with GraphPad Prism 9.0. B. Cells were incubated with drugs for 48 h (Vero) or 96 h (HAWEC-02014 and HNCEC/HL-008), then measured the cell viability by Cell Counting Kit-8 and graphed with GraphPad Prism 9.0. The IC_{50} and CC_{50} of five positive drugs in Vero, HAWEC-02014 and HNCEC/HL-008 were shown.

(MOI) of 0.01, 0.05 and 0.1. We found that all three limbal epithelial cells can be sufficiently infected by the virus and can support viral replication (Fig. 2A). More than half of limbal epithelial cells had been infected by SARS-CoV-2 at a MOI of 0.1, and limbal epithelial cells seemed to be a better host than the human airway epithelial cells as shown in Fig. 2B [27,28]. Additionally, other primary ocular epithelial cells, such as lacrimal gland, lacrimal sac, nasolacrimal duct, conjunctiva and retina, did not support SARS-CoV-2 infection and replication although ACE2 and TMPRSS2 expressed well (fig. S3A). Among the three differential limbal epithelial cells, HNCEC/HL-008 exhibited the strongest susceptivity to SARS-CoV-2 infection in spite of the lowest TMPRSS2 expression (Fig. 2B). We discovered that both limbal and bronchial epithelial cells formed quite a lot of syncytia when infected by SARS-CoV-2. We thereby co-cultured HNCEC/HL-008 and HAWEC-02014 with Spike-GFP expressed HEK293 cells or GFP alone expressed HEK293 cells. The Spike-ACE2 dependent syncytia was obviously glaring in panel with Spike-GFP expressed HEK293 cells stronger than GFP alone cells (Fig. 2C). This result suggested that limbal epithelial cells formed syncytia via spike glycoprotein, and then facilitated SARS-CoV-2 entry [29–31]. Additionally, there were slight cytopathic effect (CPE) caused by SARS-CoV-2 infection at dpi.4 of a MOI = 0.1, indicating the clinical symptoms caused by COVID-19 (fig. S3B).

3.3. Evaluation of SARS-CoV-2 variants infection of limbal

Mutations in Spike protein may influence the transmissibility, antibody escape and high vaccine breakthrough of SARS-CoV-2 [32]. We thereby infected HNCEC/HL-008 with four widely pandemic variants of SARS-CoV-2, including Delta, Omicron BA 1.1, Omicron BA 2.2 and Omicron BA 5.1. Compared to the mutant strains of Delta, BA 1.1 and BA 5.1, the tendency of Ct value in BA 2.2 showed a mild decrease (Fig. 3A). In addition, the immunofluorescence of NP reflected BA 2.2 had a lagging and ineffective infection compared to other strains (Fig. 3 B). HNCEC/HL-01038 and HNCEC/HL-01049 also displayed different preference to Delta and BA 2.2 infection, for both cells showing stronger NP expression in Delta infected group at dpi.4 (fig. S4). The expression of spike and NP at dpi.4 was measured by Western blot in Fig. 3C, and Delta strain displayed strongest infectivity among the four mutants. Due to the restriction of virus isolation and BSL-3 lab's working program, we did not detect the Omicron BA 1.1 and BA 5.1 infection in HNCEC/HL-01038 and HNCEC/HL-01049. In our previous study, the HNCEC/HL-008 proliferated rapidly for 20 population doublings in 65 days, and could be passaged steadily more than 50 population doublings (PD) [20]. Therefore, we chose HNCEC/HL-008 and Delta for subsequent drug-screening and mechanism research in consideration of its high infection efficiency.

3.4. SARS-CoV-2 infection promotes IL-6 secretion in limbal epithelial

Previous reports showed that ocular surface was a potential transmission route for SARS-CoV-2 infection, which resulted in mild symptoms such as viral conjunctivitis [33,34]. The conjunctivitis was recommended as one of symptoms and a sign predictor of COVID-19. Inflammatory cytokine storms, especially rapidly rising of IL-6 and IL-8, represented the clinical symptom progress [35]. In order to measure the inflammatory response, we infected HNCEC/HL-008 with five SARS-CoV-2 at three titers and analyzed soluble inflammatory factors in supernatant using Elisa Kit at dpi.4. We found all viral strains stimulated IL-6 secretion at different titers of infection (Fig. 4A). However, the secretion of IL-8 did not display significant increase by virus infection (Fig. 2B). In addition, the secretion of IL-18, IL-23, IL-27 and IL-33 was under the detection level of Elisa Kit both in cell supernatant and cell debris, which may be due to the tissue cells specificity (results not displayed). Based on these findings, we concluded that SARS-CoV-2 can infect limbal epithelial cells and induce slight conjunctivitis due to high IL-6 secretion.

3.5. Other protease, but not TMPRSS2 mediated SARS-CoV-2 entry in limbal

Lacrimal gland, lacrimal sac, nasolacrimal duct, conjunctiva and retina epithelial cells expressed both ACE2 and TMPRSS2, but cannot be infected by SARS-CoV-2. We therefore speculated other unknown host protein participated in the step. Camostat, a selective TMPRSS2 inhibitor, was reported to inhibit SARS-CoV-2 infection in pneumonocyte [17]. Antiviral results showed that camostat inhibited SARS-CoV-2 infection in HNCEC/HL-008 or Vero (Fig. 5A and B). Direct violet 1, an organic dye, showed tremendous inhibition of SARS-CoV-2 Pseudo-Virus entry via interacting with spike [36]. However, Direct violet 1 did not show expected inhibition in both limbal and bronchial epithelial cells. Ribavirin, ritonavir and lopinavir targeted at RdRp and 3CLpro were found to significantly inhibit infection in all three cells models (Fig. 5). Briefly, the route of SARS-CoV-2 infection in limbal was different from that in bronchial, in which TMPRSS2 mediated spike cleavage and virions entry, according to the above results. Probably other protease, but not TMPRSS2 played a dominant role when SARS-CoV-2 infected limbal.

3.6. Interferon therapy plays a pivotal role in ocular infection

The interferons were widely used as immunomodulators in viral related eye symptoms. We treated CR-cells infected by Delta strain
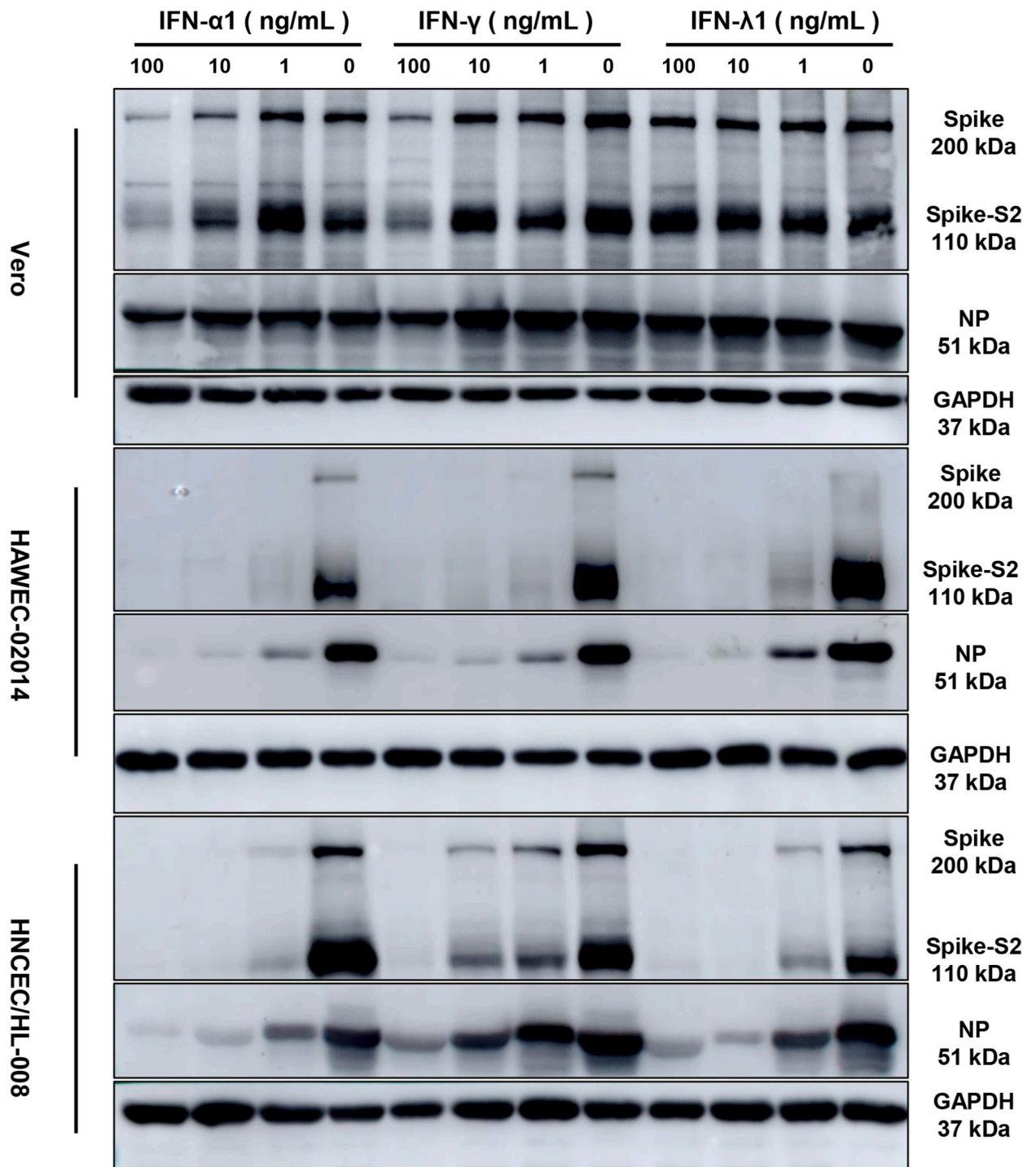
Fig. 6. Inhibition of SARS-CoV-2 infection by IFN-α1 (type I), IFN-γ (type II) and IFN-λ1 (type III) interferons in different cell models.
Vero, HAWEC-02014 and HNCEC/HL-008 cells were pretreated with diluted recombinant human IFN-α1,IFN-γ or IFN-λ1 and infected at MOI of
0.05 (Delta strain). The expression of SARS-CoV-2 spike glycoprotein, nucleocapsid, and GAPDH was evaluated by Western Blot at dpi.2 (Vero cells)
or dpi.4 (HAWEC-02014 and HNCEC/HL-008 cells). The full, non-adjusted images were displayed in the supplementary material 2 (Figure.2,
Figure.3 and 4).

with IFN-α1, IFN-γ and IFN-λ1, then estimated the therapeutic efficacy by Western blot. We observed dose dependent inhibition of NP
and Spike expression in all IFN-α1 treated cells (Fig. 6), which demonstrated the commonly therapeutic effect of IFN-α1. However, the
IFN-γ and IFN-λ1, had an alternative effect in humanized primary cells and Vero cells. HAWEC-02014 isolated from human normal

bronchial was the most sensitive to both IFN-γ and IFN-λ1, and almost 90 % of NP and spike were eliminated when treated with just 1.0 ng/mL interferons (Fig. 6). In HNCEC/HL-008, IFN-γ displayed nearly 50 % inhibition of NP at 10 ng/mL and complete elimination at 100 ng/mL. In addition, IFN-λ1 displayed a similar trend as in HAWEC-02014. Interferon-λ1 (10 ng/mL) displayed 90 % down-regulation of both NP and Spike in HNCEC/HL-008 and HAWEC-02014 infected by Delta strain (Fig. 6). However, IFN-γ and IFN-λ1 treatment did not inhibit SARS-CoV-2 infection in Vero cells for the lack of related signaling pathways. Based on our research, we thereby concluded that immune-associated drugs, such as IFN-α1, IFN-γ and IFN-λ1, showed distinct discrepancy when used in the treatment of ocular infection by SARS-CoV-2.

3.7. High-throughput antiviral drug screening in Vero and HNCEC/HL-008 cells with SARS-CoV-2 infection

To identify candidate pre-drugs against SARS-CoV-2 infection, we have screened two drug Libraries, HY-L021 and HY-L021L, in Vero and HNCEC/HL-008 cells infected with Delta viral strain at MOI = 0.05. Through three round-screening, we found fifteen compounds showed anti-viral effect in Vero and HNCEC/HL-008 cells (Table .1). In the study, four compounds were found to be effective only in Vero cells, while seven compounds showed efficacy only in HNCEC/HL-008 cells. DEHP/Bis(2-ethylhexyl) phthalate, Hygromycin B, Lasalocid sodium and Aurantio-obtusin displayed dose-dependent inhibition to SARS-CoV-2 Delta strain infection in both Vero and HNCEC/HL-008 cells. In summary, as a potential SARS-CoV-2 infection model, HNCEC/HL-008 cells provided an alternative choice for drug screening, which may contribute to finding more therapies against COVID-19 when collaborating with traditional models, such as Vero, Vero E6 or Calu-3 cells.

4. Discussion

Besides high frequency of severer virus mutation, other potential routes of viral transmission beyond the respiratory tract aggravated the COVID-19 epidemic [37]. SARS-CoV-2 enters cells via multi-receptors known as ACE2 and TMPRSS2 [38], which extensively exist in human organs [39]. Nasal cavity, lung, ocular, ileum, colon, fetal thymus, gallbladder and kidney co-express ACE2 and TMPRSS2 based on a single-cell RNA sequencing research [39,40]. The cornea and conjunctival are the regions which directly contact with external environment, making it possible for aerosol infection of viruses. Meanwhile, high expression of receptors in colon and detection of viral RNA in anal swab show potential transmission via fecal-oral [37,41]. To test the possibility of SARS-CoV-2 infection of ocular, we used CR-primary ocular epithelial cells for SARS-CoV-2 infection, and established a cell model for drug screening.

Nine cell lines from different ocular function areas were detected with high expression of ACE2 and TMPRSS2, but only epithelial cells at limbal supported infection. Meanwhile, we found that the TMPRSS2 expression was lower in all three limbal epithelial cells than other ocular areas. Moreover, TMPRSS2 antagonist Camostat showed limited effect in HNCEC/HL-008. We thereby speculate that other viral related receptors may participate in limbal infection by SARS-CoV-2. TMPRSS4 was implicated in SARS-CoV-2 infection in small intestinal enterocytes, and scRNA-seq results also showed elevated TMPRSS4 expression in limbal cells compared with central cornea, which could be a reference for its function in limbal [42,43].

When infected by SARS-CoV-2, the limbal epithelial cells displayed CPE and IL-6 rising, which reflected the injury caused by viral replication and immune responses. In addition, the non-significant secretion of IL-8 in infected or uninfected cells was attributed to the tolerance of limbal epithelium. We also measured other inflammatory factors (IL-18, IL-21, IL-27 and IL-33) in SARS-CoV-2 infected limbal epithelial cells. However, the protein secretion was under the detection level of Elisa Kit in both infected or uninfected cells. The high expression of IL-33 and other inflammatory factors were reported to be correlated with T-cell activation and lung disease severity in COVID-19 patients [44]. Therefore, in limbal epithelium cell (HCNEC/HL-008) alone, IL-33 and other inflammatory factors'

Table 1
Anti-SARS-CoV-2 screening for HY-L021P (MedChemExpress, China) in Vero and HNCEC/HL-008 cells.

	IC50/CC50 in Vero (μM)	IC50/CC50 in HNCEC/HL-008 (μM)	Reported (yes or no)	Target and Mechanism
20(S)-Hydroxycholesterol	NS	0.4–1.2/>33.3	Yes	RdRp and Mpro
Penciclovir	NS	3.7–11.1/>33.3	Yes	RdRp
alpha-Boswellic acid	NS	1.2–3.7/>33.3	Yes	Spike
Schisandrin C	NS	11.3–33.3/>100	Yes	Spike
Procyanidin C1	3.7–11.1/>33.3	NS	Yes	Mpro
Progesterone	3.7–11.1/>33.3	NS	Yes	regulation of immune responses, damage repair
Mycophenolic acid	0.4–1.2/>100	NS	Yes	Plpro (papain-like protease)
Aloperine	3.7–11.1/>33.3	NS	Yes	Spike
Dictamnine	NS	11.3–33.3/>100	No	
Syrosingopine	NS	3.7–11.1/>100	No	
Ascomycin	NS	3.7–11.1/>33.3	No	
DEHP/Bis(2-ethylhexyl) phthalate	1.2–3.7/>33.3	11.3–33.3/>100	No	
Hygromycin B	1.2–3.7/>100	0.4–1.2/>11.1	No	
Lasalocid sodium	3.7–11.1/>100	1.2–3.7/>33.3	No	
Aurantio-obtusin	3.7–11.1/>33.3	3.7–11.1/>100	No	

secretion cannot be detected for lack of immune cells. For better protecting eyes from COVID-19, we evaluated the antiviral effects of different interferons in three cells. Interferon α1, IFN λ1 and IFN-γ showed cell-specific antiviral effect in limbal and bronchial epithelial cells. Our results provided an approach to clinical therapy with interferon against SARS-CoV-2 infection. However, further studies are required to properly assess the mechanisms involving interferons mediating viral elimination in cells and animal models.

Drug development is more urgent in order to fight against COVID-19 and other diseases, which depends on rational drug design and suitable screening platforms. Because of the differences between normal human cells and immortalized cell lines, drugs screened with immortalized cells failed in further animal or clinical trials [45,46]. 3D-Cell models containing explants and organoids are the more suitable instruments, because of the affinity to mimic SARS-CoV-2 infection of human. Primary cells from respiratory tract (nasal, bronchial, bronchiolar, and alveolar tissue) have been established to perfect SARS-CoV-2 study [47,48]. In addition, Stem cells were induced to produce type 2 alveolar epithelial cells (iAT2) in an ALI (air-liquid interface) system aiming to identify gene responses to SARS-CoV-2 infection [49]. However, classical primary cell culture and ALI needed sums of cytokines and limited passage number (usually less than 10 times), which limited its use for drug screening. In our study, CR-HCNEC/HL-008 proliferated rapidly and doubled every three days, and these cells can be passaged steadily more than 50 population doublings [20], which made it possible for large scale experiments. Comparing the infection efficiency of three limbal epithelial cells, we chose HCNEC/HL-008 as screening model. Candidate drugs screened from libraries HY-L021 and HY-L021L respectively in Vero and HCNEC/HL-008 differed a lot, manifesting the necessity of multifarious models.

In conclusion, the data presented in this study showed that the limbal epithelial cells are susceptible to SARS-CoV-2 infection, and the eye surface can be considered as a potential transmission route. SARS-CoV-2 may infect limbal through other unknown receptors beyond ACE2 and TMPRSS2, which can be absolutely inhibited by interferon treatment. Further studies are warranted to better understand ocular infection associated to conjunctivitis symptoms and how virus in eyes spread to other regions of the body.

5. Conclusion

This research reveal important commonalities between COVID-19 and ocular infection with SARS-CoV-2, and establish an ideal cell model for drug screening and mechanism research. We found that SARS-CoV-2 infected limbal epithelial cells efficiently, and caused cytopathic effects and inflammatory cytokine secretion. Interferon therapy significantly inhibited viral infection in both limbal and bronchial epithelial cells. Additionally, drug screening in Vero or limbal cell models displayed discrepant results. In conclusion, the data showed that the limbal epithelial cells are susceptible to SARS-CoV-2 infection through other unknown receptors beyond ACE2 and TMPRSS2, and the ocular surface can be considered as a potential transmission route.

Limitations of study

Although we have found compelling evidence that limbal epithelial cells can be effortlessly infected with SARS-CoV-2, this study has some clear limitations. First, we obtained each ocular cell type only from one to three donors. Second, we cannot verify ocular infection is a route for SARS-CoV-2 infection directly, for aerosol droplets assay was not conducted. Third, about drug screening difference, we attributed it to cell specificity, but further research is required to elaborate which gene and pathway contribute to the distinction.

Data availability

The data associated with this study was not deposited into a publicly available repository. All data associated with this study have been present in the paper or supplementary materials. Data will be made available on request.

CRediT authorship contribution statement

Yu Xiao: Writing – original draft, Supervision, Methodology, Investigation, Formal analysis, Data curation. **Ling Wang:** Project administration, Methodology, Investigation. **Shi-xu Li:** Methodology, Investigation. **Shi-song Fang:** Resources, Funding acquisition. **Fan Luo:** Writing – review & editing, Formal analysis, Data curation. **Shu-liang Chen:** Writing – review & editing, Data curation. **Xuan Zou:** Resources. **Lin Ye:** Writing – review & editing, Resources, Methodology, Investigation. **Wei Hou:** Writing – review & editing, Supervision, Resources, Project administration, Funding acquisition.

Declaration of competing interest

Acknowledgements

Appendix A. Supplementary data

Supplementary data to this article can be found online at https://doi.org/10.1016/j.heliyon.2024.e30044.

Vero and HNCEC/HL-008 cells were incubated with a series dilution of drugs and infected with Delta strain at MOI of 0.05, then immunoblotted with antibody against nucleocapsid of SARS-CoV-2 and strained with DAPI at dpi.2 (Vero cells) or dpi.4 (HNCEC/HL-008 cells). The final results were summarized in this table, and the research progress of these potential drugs were evaluated through *National Library of Medicine*.

References

[1] P. V'Kovski, A. Kratzel, S. Steiner, H. Stalder, V. Thiel, Coronavirus biology and replication: implications for SARS-CoV-2, Nat. Rev. Microbiol. 19 (3) (2021) 155–170.

[2] G.B.D.D. Collaborators, Global age-sex-specific mortality, life expectancy, and population estimates in 204 countries and territories and 811 subnational locations, 1950-2021, and the impact of the COVID-19 pandemic: a comprehensive demographic analysis for the Global Burden of Disease Study 2021, Lancet. (2024). S0140-6736(24)00476-8.

[3] V.O. Puntmann, S. Martin, A. Shchendrygina, J. Hoffmann, M.M. Ka, E. Giokoglu, B. Vanchin, N. Holm, A. Karyou, G.S. Laux, C. Arendt, P. De Leuw, K. Zacharowski, et al., Long-term cardiac pathology in individuals with mild initial COVID-19 illness, Nat. Med. 28 (10) (2022, Oct) 2117–2123.

[4] Y. Geng, Y. Wang, Stability and transmissibility of SARS-CoV-2 in the environment, J. Med. Virol. 95 (1) (2022, Jan) e28103.

[5] N.H.L. Leung, Transmissibility and transmission of respiratory viruses, Nat. Rev. Microbiol. 19 (8) (2021) 528–545.

[6] Y. Yan, B. Diao, Y. Liu, W. Zhang, G. Wang, X. Chen, Severe Acute respiratory syndrome coronavirus 2 nucleocapsid protein in the ocular tissues of a patient previously infected with coronavirus disease 2019, JAMA Ophthalmol 138 (11) (2020) 1201–1204.

[7] O.B. Sawant, S. Singh, R.E. Wright 3rd, K.M. Jones, M.S. Titus, E. Dennis, E. Hicks, P.A. Majmudar, A. Kumar, S.I. Mian, Prevalence of SARS-CoV-2 in human post-mortem ocular tissues, Ocul. Surf. 19 (2021) 322–329.

[8] Y. Zhou, C. Duan, Y. Zeng, Y. Tong, Y. Nie, Y. Yang, Z. Chen, C. Chen, Ocular findings and proportion with conjunctival SARS-COV-2 in COVID-19 patients, Ophthalmology 127 (7) (2020) 982–983.

[9] J. Xia, J. Tong, M. Liu, Y. Shen, D. Guo, Evaluation of coronavirus in tears and conjunctival secretions of patients with SARS-CoV-2 infection, J. Med. Virol. 92 (6) (2020) 589–594.

[10] M. Ozturk, D. Kumova, S. Alacam, H. Erdogan, F. Onder, Detection of coronavirus in tear samples of hospitalized patients with COVID-19, Int. Ophthalmol. 43 (2) (2022, Feb) 451–462.

[11] A. Tajima, Y. Sassa, D. Ishio, S. Yamashita, E. Sadashima, R. Arai, K. Iwanaga, S. Yoshida, K.H. Sonoda, H. Enaida, Clinical features of 26 cases of COVID-19-associated conjunctivitis, Jpn. J. Ophthalmol. 68 (1) (2024) 57–63.

[12] E. Niedzwiecka, San Miguel MP. Canto, M. Gonzalez Herrera, I. Sanchez Rodriguez-Acosta, Bilateral Acute depigmentation of the Iris (BADI) following covid-19 infection, Ocul. Immunol. Inflamm. (2022) 1–2.

[13] H. Ji, Y. Yang, Y. Lu, X. Kong, G. Yang, J. Liu, Y. Yang, X. Wang, X. Ma, Prevalence of dry eye during the COVID-19 pandemic: a systematic review and meta-analysis, PLoS One 18 (12) (2023) e0288523.

[14] C. Gronbeck, A. Grzybowski, J.M. Grant-Kels, COVID-19 and the eye, Clin. Dermatol. 42 (1) (2024 Jan-Feb) 17–24.

[15] N. Sidhu, M. Vanathi, N. Gupta, R. Tandon, COVID and COVID vaccine-related corneal morbidity: a review, Indian J. Ophthalmol. 71 (12) (2023) 3595–3599.

[16] T.P.H. Lin, M. Sen, V. Gupta, R. Agrawal, P. Lanzetta, G. Giannaccare, C.K.M. Chan, K. Agrawal, N.K. Menia, W. Rojas-Carabali, A. Arora, D. Martinuzzi, A. Taloni, et al., Update on coronavirus disease 2019: ophthalmic manifestations and adverse reactions to vaccination, Asia-Pacific journal of ophthalmology 12 (6) (2023) 512–536.

[17] M. Hoffmann, H. Kleine-Weber, S. Schroeder, N. Kruger, T. Herrler, S. Erichsen, T.S. Schiergens, G. Herrler, N.H. Wu, A. Nitsche, M.A. Muller, C. Drosten, S. Pohlmann, SARS-CoV-2 cell entry depends on ACE2 and TMPRSS2 and is blocked by a clinically proven protease inhibitor, Cell 181 (2) (2020) 271–280 e278.

[18] N. Palechor-Ceron, E. Krawczyk, A. Dakic, V. Simic, H. Yuan, J. Blancato, W. Wang, F. Hubbard, Y.L. Zheng, H. Dan, S. Strome, K. Cullen, B. Davidson, et al., Conditional reprogramming for patient-derived cancer models and next-generation living biobanks, Cells 8 (11) (2019).

[19] X. Liu, E. Krawczyk, F.A. Suprynowicz, N. Palechor-Ceron, H. Yuan, A. Dakic, V. Simic, Y.L. Zheng, P. Sripadhan, C. Chen, J. Lu, T.W. Hou, S. Choudhury, et al., Conditional reprogramming and long-term expansion of normal and tumor cells from human biospecimens, Nat. Protoc. 12 (2) (2017) 439–451.

[20] L. Wang, L. Ye, G. Wei, Y. Chen, L. Ye, X. Wu, Z. Zeng, Y. Wang, G. Yin, X. Long, H. Li, Conditional reprogrammed human limbal epithelial cells represent a novel in vitro cell model for drug responses, Biochemical and biophysical research communications 499 (4) (2018) 735–742.

[21] H. Xia, Z. Cao, X. Xie, X. Zhang, J.Y. Chen, H. Wang, V.D. Menachery, R. Rajsbaum, P.Y. Shi, Evasion of type I interferon by SARS-CoV-2, Cell Rep. 33 (1) (2020) 108234.

[22] L. Wang, S. Li, K. Cai, Y. Xiao, L. Ye, TLR7 agonists modulate the activation of human conjunctival epithelial cells induced by IL-1 beta via the ERK1/2 signaling pathway, Inflammation 46 (4) (2023) 1430–1444.

[23] Z. Zhang, Q. Bai, Y. Chen, L. Ye, X. Wu, L. Long, L. Ye, J. Liu, H. Li, Conditionally reprogrammed human normal bronchial epithelial cells express comparable levels of cytochromes p450 and are sensitive to BaP induction, Biochemical and biophysical research communications 503 (3) (2018) 2132–2138.

[24] Liu Rong, Tan Yongyao, Li Guigang, Luo Ban, Hu Weikun, Immunohistological study of human lacrimal mucosa and epithelial stem cells in different parts of lacrimal duct, Acta Med Univ Sci Technol Huazhong 51 (1) (2022) 63–67, 2022; 51(01):63-67.

[25] K. Kitazawa, S. Deinhardt-Emmer, T. Inomata, S. Deshpande, C. Sotozono, The transmission of SARS-CoV-2 infection on the ocular surface and prevention strategies, Cells 10 (4) (2021).

[26] F. Aiello, G. Gallo Afflitto, R. Mancino, J.O. Li, M. Cesareo, C. Giannini, C. Nucci, Coronavirus disease 2019 (SARS-CoV-2) and colonization of ocular tissues and secretions: a systematic review, Eye (Lond). 34 (7) (2020) 1206–1211.

[27] I. Djidrovski, M. Georgiou, G.L. Hughes, E.I. Patterson, A. Casas-Sanchez, S.H. Pennington, G.A. Biagini, M. Moya-Molina, J. van den Bor, M.J. Smit, G. Chung, M. Lako, L. Armstrong, SARS-CoV-2 infects an upper airway model derived from induced pluripotent stem cells, Stem Cell. 39 (10) (2021) 1310–1321.

[28] A.Z. Mykytyn, T.I. Breugem, S. Riesebosch, D. Schipper, P.B. van den Doel, R.J. Rottier, M.M. Lamers, B.L. Haagmans, SARS-CoV-2 entry into human airway organoids is serine protease-mediated and facilitated by the multibasic cleavage site, Elife 10 (2021).

[29] S. Xia, M. Liu, C. Wang, W. Xu, Q. Lan, S. Feng, F. Qi, L. Bao, L. Du, S. Liu, C. Qin, F. Sun, Z. Shi, et al., Inhibition of SARS-CoV-2 (previously 2019-nCoV) infection by a highly potent pan-coronavirus fusion inhibitor targeting its spike protein that harbors a high capacity to mediate membrane fusion, Cell Res. 30 (4) (2020) 343–355.

[30] L. Lu, Q. Liu, Y. Zhu, K.H. Chan, L. Qin, Y. Li, Q. Wang, J.F. Chan, L. Du, F. Yu, C. Ma, S. Ye, K.Y. Yuen, et al., Structure-based discovery of Middle East respiratory syndrome coronavirus fusion inhibitor, Nat. Commun. 5 (2014) 3067.

[31] H. Ma, Z. Zhu, H. Lin, S. Wang, P. Zhang, Y. Li, L. Li, J. Wang, Y. Zhao, J. Han, Pyroptosis of syncytia formed by fusion of SARS-CoV-2 spike and ACE2-expressing cells, Cell Discov 7 (1) (2021) 73.

[32] C.B. Jackson, M. Farzan, B. Chen, H. Choe, Mechanisms of SARS-CoV-2 entry into cells, Nat. Rev. Mol. Cell Biol. 23 (1) (2022) 3–20.

[33] A.A. Panoutsopoulos, Conjunctivitis as a sentinel of SARS-CoV-2 infection: a need of revision for mild symptoms, SN Compr Clin Med 2 (7) (2020) 859–864.

[34] L.W. Lim, G.S. Tan, V. Yong, D.E. Anderson, D.C. Lye, B. Young, R. Agrawal, Acute onset of bilateral follicular conjunctivitis in two patients with confirmed SARS-CoV-2 infections, Ocul. Immunol. Inflamm. 28 (8) (2020) 1280–1284.

[35] M. Ranzenigo, E. Bruzzesi, L. Galli, A. Castagna, G. Ferrari, Symptoms and signs of conjunctivitis as predictors of disease course in COVID-19 syndrome, J Ophthalmic Inflamm Infect 11 (1) (2021) 35.

[36] D. Bojadzic, O. Alcazar, J. Chen, S.T. Chuang, J.M. Condor Capcha, L.A. Shehadeh, P. Buchwald, Small-molecule inhibitors of the coronavirus spike: ACE2 protein-protein interaction as blockers of viral attachment and entry for SARS-CoV-2, ACS Infect. Dis. 7 (6) (2021) 1519–1534.

[37] X.J. Meng, T.J. Liang, SARS-CoV-2 infection in the gastrointestinal tract: fecal-oral route of transmission for COVID-19? Gastroenterology 160 (5) (2021) 1467–1469.

[38] L. Zhang, M. Mann, Z.A. Syed, H.M. Reynolds, E. Tian, N.L. Samara, D.C. Zeldin, L.A. Tabak, K.G. Ten Hagen, Furin cleavage of the SARS-CoV-2 spike is modulated by O-glycosylation, Proc Natl Acad Sci U S A. 118 (47) (2021).

[39] W. Sungnak, N. Huang, C. Becavin, M. Berg, R. Queen, M. Litvinukova, C. Talavera-Lopez, H. Maatz, D. Reichart, F. Sampaziotis, K.B. Worlock, M. Yoshida, J. L. Barnes, et al., SARS-CoV-2 entry factors are highly expressed in nasal epithelial cells together with innate immune genes, Nature medicine 26 (5) (2020) 681–687.

[40] L. Fodoulian, J. Tuberosa, D. Rossier, M. Boillat, C. Kan, V. Pauli, K. Egervari, J.A. Lobrinus, B.N. Landis, A. Carleton, I. Rodriguez, SARS-CoV-2 receptors and entry genes are expressed in the human olfactory neuroepithelium and brain, iScience 23 (12) (2020) 101839.

[41] M. Szczesniak, J. Brydak-Godowska, SARS-CoV-2 and the eyes: a review of the literature on transmission, detection, and ocular manifestations, Med Sci Monit 27 (2021) e931863.

[42] R. Zang, M.F. Gomez Castro, B.T. McCune, Q. Zeng, P.W. Rothlauf, N.M. Sonnek, Z. Liu, K.F. Brulois, X. Wang, H.B. Greenberg, M.S. Diamond, M.A. Ciorba, S.P. J. Whelan, et al., TMPRSS2 and TMPRSS4 promote SARS-CoV-2 infection of human small intestinal enterocytes, Science immunology 5 (47) (2020).

[43] A.Z. Eriksen, R. Moller, B. Makovoz, S.A. Uhl, B.R. tenOever, T.A. Blenkinsop, SARS-CoV-2 infects human adult donor eyes and hESC-derived ocular epithelium, Cell Stem Cell 28 (7) (2021) 1205–1220 e1207.

[44] F. Furci, G. Murdaca, A. Allegra, L. Gammeri, G. Senna, S. Gangemi, IL-33 and the cytokine storm in COVID-19: from a potential immunological relationship towards precision medicine, Int. J. Mol. Sci. 23 (23) (2022).

[45] R.B. Rosa, W.M. Dantas, J.C.F. do Nascimento, M.V. da Silva, R.N. de Oliveira, L.J. Pena, In vitro and in vivo models for studying SARS-CoV-2, the etiological agent responsible for COVID-19 pandemic, Viruses 13 (3) (2021).

[46] M. Hoffmann, K. Mosbauer, H. Hofmann-Winkler, A. Kaul, H. Kleine-Weber, N. Kruger, N.C. Gassen, M.A. Muller, C. Drosten, S. Pohlmann, Chloroquine does not inhibit infection of human lung cells with SARS-CoV-2, Nature 585 (7826) (2020) 588–590.

[47] N. Zhu, W. Wang, Z. Liu, C. Liang, W. Wang, F. Ye, B. Huang, L. Zhao, H. Wang, W. Zhou, Y. Deng, L. Mao, C. Su, et al., Morphogenesis and cytopathic effect of SARS-CoV-2 infection in human airway epithelial cells, Nat. Commun. 11 (1) (2020) 3910.

[48] F.S. Varghese, E. van Woudenbergh, G.J. Overheul, M.J. Eleveld, L. Kurver, N. van Heerbeek, A. van Laarhoven, P. Miesen, G. den Hartog, M.I. de Jonge, R. P. van Rij, Berberine and obatoclax inhibit SARS-cov-2 replication in primary human nasal epithelial cells in vitro, Viruses 13 (2) (2021).

[49] X. Liu, Y. Wu, L. Rong, Conditionally reprogrammed human normal airway epithelial cells at ALI: a physiological model for emerging viruses, Virol. Sin. 35 (3) (2020) 280–289.